Numerical computations of fundamental eigenstates for the Schrödinger operator under constant magnetic field

François Alouges*and Virginie Bonnaillie Noël†

Abstract

Motivated by questions arising in the theory of superconductivity, we are interested in the study of the fundamental state of the Schrödinger operator with magnetic field in a domain with corners. Although this problem has been extensively studied theoretically, much less papers deal with numerical approaches. In this paper, we propose numerical experiments based on the finite element method to determine the bottom of the spectrum of the operator. Analyzing the drawbacks of a standard method and the properties of the operator, we propose a natural gauge-invariant method and provide a few numerical simulations. We furthermore improve the numerical results by coupling the method with a mesh-refinement technique based on a posteriori error estimates developed in [4]. This allows us to look at the monotonicity of the smallest eigenvalue in an angular sector with respect to the angle, which complement the theoretical study of [3].

1 Physical motivation and mathematical known results

A superconducting sample cooled below a certain critical temperature T_C carries current without loss, letting it flow without any resistance. This explains the increasing interest of such materials for experimental engineering. Another characteristic is the expelling of any magnetic field, that is to say a superconductor sample will not allow a magnetic field to penetrate in its interior. This effect, called the Meissner Effect, occurs only for relatively small magnetic fields. If the magnetic field becomes too large, the sample loses its superconducting behavior by penetration of the external magnetic field, it is the "normal state".

*Université Paris XI, Laboratoire de Mathématique, UMR CNRS 8628, 91405 Orsay Cedex, France, Francois.Alouges@math.u-psud.fr

†ENS Cachan, Antenne de Bretagne, IRMAR, UMR CNRS 6625, 35042 Bruz, France, Virginie.Bonnaillie@bretagne.ens-cachan.fr

Two kinds of superconductors are distinguished. Type I superconductors directly switch between the normal state and the superconductor state with Meissner effect. On the other hand, Type II superconductors pass from the normal state to the superconductor state with Meissner effect by going through a "mixed state" where the external magnetic field penetrates the sample in vortices. The number of such vortices increases with the magnitude of the external magnetic field and they eventually fill up the sample. This phenomenon was described by the Ginzburg-Landau theory developed by De Gennes [10] and Tinkham [21].
We consider a Type II cylindrical superconducting sample, denoting by $\Omega \subset \mathbb{R}^2$ its cross section and apply a magnetic field $\mathcal{H}$ along the cylindrical axis. In the sequel, we will consider Ω to be a curvilinear polygon whose vertices are denoted by $S_1, \ldots, S_N$ with corresponding angles $\alpha_1, \ldots, \alpha_N$. Then, up to renormalization factors, the free energy writes

$$\mathcal{G}(\psi, \mathcal{A}) = \frac{1}{2} \int_\Omega \left\{ |(\nabla - i\kappa\mathcal{A})\psi|^2 + \kappa^2 |\mathrm{curl}\, \mathcal{A} - \mathcal{H}|^2 + \frac{\kappa^2}{2}(|\psi|^2 - 1)^2 \right\} dx. \tag{1}$$

The superconducting properties are described by the minimizers $(\psi, \mathcal{A})$ of this Ginzburg-Landau functional $\mathcal{G}$. More precisely, the complex-valued function ψ is the order parameter and the magnitude $|\psi|^2$ gives the density of superconducting electrons, the phase of ψ determining the current flow. In the normal state, $\psi \simeq 0$ and in the superconducting state, $|\psi| \simeq 1$. The vector field $\mathcal{A}$ defined on $\mathbb{R}^2$ is the magnetic potential and $B = \mathrm{curl}\, \mathcal{A}$ is the induced magnetic field. The two remaining parameters in the free energy (1) are the magnitude $\mathcal{H}$ of the applied magnetic field, assumed to be constant in space and κ the so-called "Ginzburg-Landau parameter". Type I superconductors correspond to $\kappa < \frac{1}{\sqrt{2}}$, and type II to $\kappa > \frac{1}{\sqrt{2}}$. From now on, we assume κ is large.

It is easily checked that the Ginzburg-Landau functional is gauge invariant according to the gauge transformation

$$\psi \to \psi e^{i\kappa\phi}, \text{ and } \mathcal{A} \to \mathcal{A} + \nabla\phi, \tag{2}$$

for any function ϕ called hereafter the gauge.
Revelant physical quantities are also gauge invariant, for instance the magnitude $|\psi|^2$, the magnetic field B, and the superconducting current $j := -\frac{i}{2\kappa}(\overline{\psi}\nabla\psi - \psi\nabla\overline{\psi}) - |\psi|^2\mathcal{A}$. In particular, if $\psi = 0$ then $j = 0$ which means that the superconductivity is destroyed and there is no supercurrent.

Critical points of the Ginzburg-Landau functional (1) satisfy the following Euler equations (cf. [14, 10]) where Γ' is the set of the boundary where the unit outward normal ν is well defined and where we have denoted

$\mathrm{curl}^{\,2}\mathcal{A} = (\partial_2(\mathrm{curl}\,\mathcal{A}), -\partial_1(\mathrm{curl}\,\mathcal{A}))$.

$$\left\{\begin{array}{rcll} -(\nabla - i\mathcal{A})^2\psi &=& \kappa^2(1-|\psi|^2)\psi, & \text{in } \Omega, \\ \mathrm{curl}^{\,2}\mathcal{A} &=& -\dfrac{i}{2\kappa}(\overline{\psi}\nabla\psi - \psi\nabla\overline{\psi}) - |\psi|^2\mathcal{A} + \mathrm{curl}\,\mathcal{H}, & \text{in } \Omega, \\ \dfrac{\partial\psi}{\partial\nu} - i\kappa\mathcal{A}\psi\cdot\nu &=& 0, & \text{in } \Gamma', \\ \mathrm{curl}\,\mathcal{A} - \mathcal{H} &=& 0, & \text{in } \partial\Omega. \end{array}\right. \tag{3}$$

The analysis of the Hessian of the functional $\mathcal{G}$ around the normal state ($\psi = 0$, $\mathcal{A}$ = external magnetic potential) leads to estimate the fundamental state for the Neumann realization of the Schrödinger operator. Namely, we define the sesquilinear form $p_{\mathcal{A},\Omega}$ in

$$H^1_{\mathcal{A}}(\Omega) = \{u \in L^2(\Omega) | (\nabla - i\mathcal{A})u \in (L^2(\Omega))^2\}, \tag{4}$$

by

$$p_{\mathcal{A},\Omega}(u,v) = \int_\Omega (\nabla - i\mathcal{A})u \cdot \overline{(\nabla - i\mathcal{A})v}\; dx,\ \forall u, v \in H^1_{\mathcal{A}}(\Omega). \tag{5}$$

We note that when Ω is bounded, then $H^1_{\mathcal{A}}(\Omega) = H^1(\Omega)$. The sesquilinear form $p_{\mathcal{A},\Omega}$ admits a unique self-adjoint extension $P_{\mathcal{A},\Omega} := -(\nabla - i\mathcal{A})^2$ defined on the domain

$$\mathcal{D}^N(P_{\mathcal{A},\Omega}) := \{u \in H^1_{\mathcal{A}}(\Omega) |\ (\nabla - i\mathcal{A})^2 u \in L^2(\Omega),\ \nu\cdot(\nabla - i\mathcal{A})u_{|_{\Gamma'}} = 0\}.$$

Our goal is to determine the fundamental state for the operator $P_{\mathcal{A},\Omega}$. The weak formulation of this problem reads

$$\begin{array}{c} \text{Find } (\mu, u) \in \mathbb{R}\times H^1_{\mathcal{A}}(\Omega), \quad ||u|| = 1 \text{ and } \mu \text{ as small as possible s.t.} \\ p_{\mathcal{A},\Omega}(u,v) = \mu\langle u, v\rangle,\ \forall v \in H^1_{\mathcal{A}}(\Omega), \end{array} \tag{6}$$

where $\langle\cdot,\cdot\rangle$ and $||\cdot||$ denote respectively the L^2-scalar product and the L^2-norm on Ω.

Remark 1.1. *Since the energy $\mathcal{G}$ is gauge invariant, for any $\phi \in H^2(\Omega)$, the operators $P_{\mathcal{A},\Omega}$ and $P_{\mathcal{A}+\nabla\phi,\Omega}$ are unitary equivalent. Furthermore, (μ, u) belongs to the spectrum of $P_{\mathcal{A},\Omega}$ if and only if $(\mu, ue^{i\phi})$ belongs to the spectrum of $P_{\mathcal{A}+\nabla\phi,\Omega}$.*

This remark shows that the bottom of the spectrum of $P_{\mathcal{A},\Omega}$ only depends on the magnetic field $B = \mathrm{curl}\,\mathcal{A}$. We therefore denote it by $\mu(B,\Omega)$. Furthermore, setting

$$\mathcal{A}_0(x) = \frac{1}{2}(x_2, -x_1), \tag{7}$$

a potential which induces a unit magnetic field, and considering any potential $\mathcal{A}$ with constant magnetic field B, then the operators $P_{\mathcal{A},\Omega}$ and $P_{B\mathcal{A}_0,\Omega}$ possess the same spectrum.

Due to the min-max principle, $\mu(B,\Omega)$ is equal to

$$\mu(B,\Omega) = \inf_{u\in H^1_{\mathcal{A}}(\Omega), u\neq 0} \frac{\displaystyle\int_\Omega |(\nabla - i\mathcal{A})u|^2 \, dx}{\displaystyle\int_\Omega |u|^2 \, dx} \text{ for any } \mathcal{A} \text{ s. t. } \operatorname{curl}\mathcal{A} = B. \quad (8)$$

A lot of papers [12, 13, 14, 17, 18] deal with estimates of $\mu(B,\Omega)$ and localization of the fundamental state in regular domains; particularly Helffer-Morame [12, 13] prove the localization of the fundamental state on the boundary and more precisely at points of maximal curvature. We want to carry on their analysis by determining the effects of a non regular boundary. Some results are announced by the Physicists Brosens, Devreese, Fomin, Moshchalkov, Schweigert and Peeters in [9, 11, 20] but not proved. Jadallah [16] and Pan [19] study the right corner situation. A more general theoretical analysis about the sector in $\mathbb{R}^2$ is proposed by Bonnaillie in [3], whereas the case of polygonal domains is considered by Bonnaillie Noël-Dauge in [5]. A partition of identity and a change of variables reduce the study of $P_{\mathcal{A},\Omega}$ for any curvilinear domain Ω to the study of three model operators

$$P_{\mathcal{A}_0,\mathbb{R}^2},\ P_{\mathcal{A}_0,\mathbb{R}\times\mathbb{R}^+} \text{ and } P_{\mathcal{A}_0,\Omega_\alpha}, \quad (9)$$

where $\Omega_\alpha := \left\{x\in\mathbb{R}^2 |\ x_1 > 0, |x_2| < \tan\frac{\alpha}{2}x\right\}$ is the sector in $\mathbb{R}^2$ with angle $\alpha \in (0, 2\pi]$. We denote more lightly by $\mu(\alpha) = \mu(1,\Omega_\alpha)$. A result in [3, 5] states that the first eigenfunction of $P_{B\mathcal{A}_0,\Omega}$ is exponentially localized in corners S_j where $\mu(\alpha_j)$ is minimum.
This present paper is devoted to the numerical computation of $\mu(\alpha)$ and illustrates the localization of the eigenfunction in any domain. For the numerical treatment of the problem, we restrict our study to potentials $\mathcal{A}$ with constant magnetic field and, due to gauge invariance (Remark 1.1), we assume that $\mathcal{A} = B\mathcal{A}_0$. The exponential localization in some points of the boundary makes the numerical treatment particularly difficult. We also quote that another numerical approach is proposed in [15] by using a boundary integral formulation, though it is restricted to regular domains.

This article is organized as follows. In Section 2, we first recall some easy invariance properties of $P_{\mathcal{A}_0,\Omega}$. These properties can explain why the standard method consisting in constructing the stiffness and mass matrices and computing the generalized eigenvalues, is inefficient for this problem. This convinces us to propose a more robust method respecting invariance properties. In Section 3, the accuracy of the method is improved by using a posteriori error estimator provided by [4]. In the last section, we implement this method to compute $\mu(\alpha)$ and see its monotonic bevahior according to the angle α. We also test the robustness of the method on several domains to illustrate known theoretical results [13, 3, 2].

2 Numerical discretization

We quickly present classical properties of the spectrum of $P_{B\mathcal{A}_0,\Omega}$. These properties can easily be justified by change of variables and construction of an unitary transformation.

Remark 2.1.

1. *Let Ω be a domain invariant under dilatation, then the spectrum of $P_{B\mathcal{A}_0,\Omega}$ is obtained from the spectrum of $P_{\mathcal{A}_0,\Omega}$ by multiplying it by B.*

2. *Denoting $\Omega_t := \{y \in \mathbb{R}^2 | y - t \in \Omega\}$ the domain deduced from Ω after translation by t. Then the operators $P_{B\mathcal{A}_0,\Omega}$ and $P_{B\mathcal{A}_0,\Omega_t}$ are unitary equivalent. Furthermore, u is an eigenvector for $P_{B\mathcal{A}_0,\Omega}$ associated with the eigenvalue μ if and only if u_t defined on Ω_t by*

$$u_t(y) := e^{i\frac{B}{2}y\wedge t}\ u(y-t) \tag{10}$$

   is an eigenvector associated with the eigenvalue μ for $P_{B\mathcal{A}_0,\Omega_t}$.

3. *Let $\Omega^\eta := \{\rho e^{i\phi} \in \mathbb{R}^2 |\ \rho e^{i(\phi-\eta)} \in \Omega\}$ be the domain deduced from Ω after a rotation of angle η. Then the two operators $P_{B\mathcal{A}_0,\Omega}$ and $P_{B\mathcal{A}_0,\Omega^\eta}$ have the same smallest eigenvalue and the eigenfunctions are deduced one from the other by a change of variables.*

We now present the classical finite element discretization of the problem. Denoting by $\mathcal{T}_h$ a triangulation of Ω and $\mathbb{P}^k(\mathcal{T}_h)$ or $\mathbb{P}^k$ the triangular elements based on polynomials of degree k, the discrete formulation associated to (6) consists in finding $(\mu_h, u_h) \in \mathbb{R} \times \mathbb{P}^k(\mathcal{T}_h)$ with μ_h as small as possible and

$$\int_\Omega |u_h|^2\ dx = 1, \tag{11}$$

$$p_{\mathcal{A},\Omega}(u_h, v_h) = \mu_h \langle u_h, v_h\rangle, \quad \forall v_h \in \mathbb{P}^k(\mathcal{T}_h). \tag{12}$$

Calling $(\phi_j)_j$ the basis functions, and writing $u_h = \sum_j u_j\phi_j$, with $u_j \in \mathbb{C}$, (12) reduces to

$$\forall k,\ \sum_j u_j\ p_{\mathcal{A},\Omega}(\phi_j, \phi_k) = \mu_h \sum_j u_j \langle \phi_j, \phi_k\rangle. \tag{13}$$

When considering the mass and stiffness matrices M and A defined by

$$M_{j,k} = \langle \phi_j, \phi_k\rangle \quad \text{and} \quad A_{j,k} = p_{\mathcal{A},\Omega}(\phi_j, \phi_k),$$

the problem becomes to find the smallest generalized eigenvalue μ_h for (A, M) and its corresponding normalized eigenvector $U = (u_j)_j$

$$AU = \mu_h MU \text{ and } {}^tUMU = 1. \tag{14}$$

Remark 2.2. *The formulation (14) is not gauge invariant. Indeed, if u is piecewise polynomial, then for any linear ϕ, $e^{i\phi}u$ is not, and does not belong to the discrete space.*

To see the effect of a translation, we consider a mesh $\mathcal{T}_h^0$ of a domain Ω of diameter comparable to unity and construct meshes $\mathcal{T}_h^j$ deduced from $\mathcal{T}_h^0$ by a translation of vectors $\mathbf{t_j} = (j, 0)$ for $j = 1, 2$. We denote by (μ^j, u^j), (μ_h^j, u_h^j) respectively the solutions of the continuous problem (6) on Ω^j with $\Omega^0 = \Omega$ and of the discrete problem (14) computed on each mesh $\mathcal{T}_h^j$ with smallest possible μ^j and μ_h^j for $j = 0, 1, 2$. According to Remark 2.1, we have for $j = 1, 2$

$$\left\{ \begin{array}{rcl} \mu^j & = & \mu^0, \\ u^j(x) & = & e^{i\frac{B}{2}x\wedge\mathbf{t_j}}u^0(x - \mathbf{t_j}),\ \forall x \in \Omega^j. \end{array} \right. \tag{15}$$

We consider two initial meshes with respectively 138 and 1328 elements, see Figure 1 and we successively apply a magnetic field of magnitude $B = 10$, 30, 50. Table 1 gives the energy computed on each mesh.

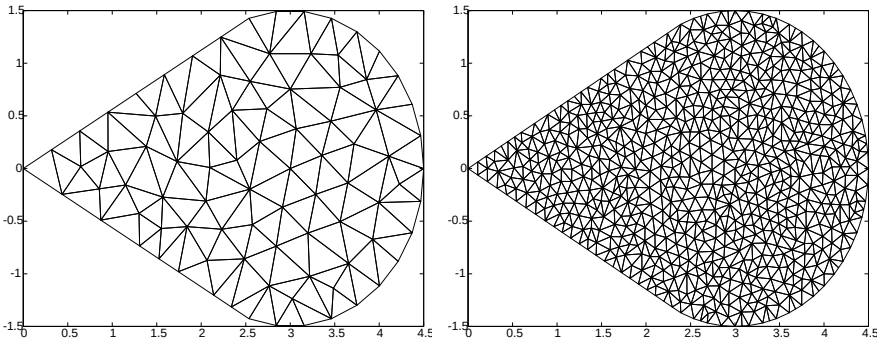

Figure 1: The domain Ω meshed with 138 and 1328 elements.

B	Mesh with 138 elements			Mesh with 1328 elements		
	μ_h^0	μ_h^1	μ_h^2	μ_h^0	μ_h^1	μ_h^2
$B = 10$	4.3306	4.2551	5.4980	4.1860	4.1810	4.2330
$B = 30$	14.3868	18.1965	30.2870	12.6555	12.9483	20.3891
$B = 50$	27.6519	43.7395	51.1149	21.3263	26.7383	47.5876

Table 1: Smallest eigenvalues computed on translated meshes.

The results presented in Table 1 do not agree with Remark 2.1, we see an increase of the eigenvalue ($B = 50$) and a dramatic change in the shape of the eigenvector with respect to the translation. For small magnetic fields

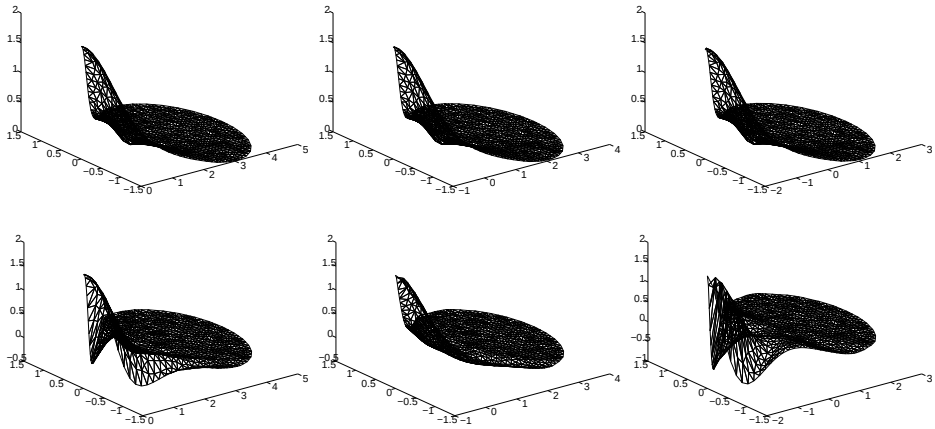

Figure 2: Modulus and real part of the fundamental state associated with translated meshes at 1328 elements, $B = 10$.

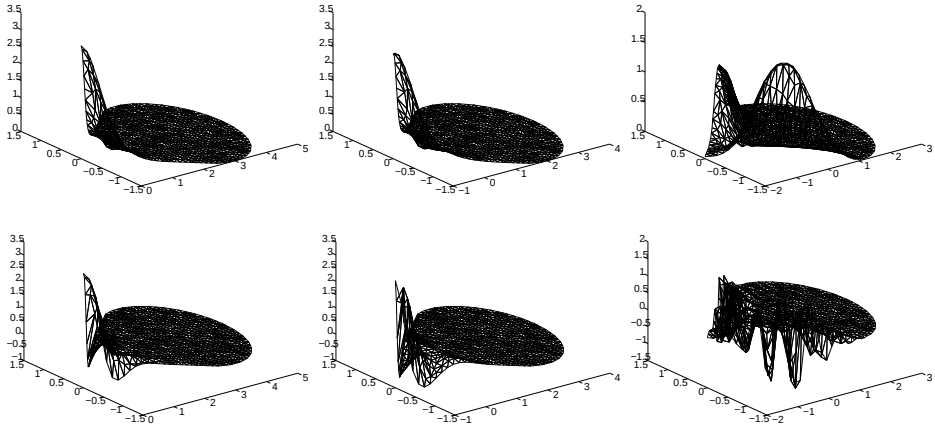

Figure 3: Modulus and real part of the fundamental state associated with translated meshes at 1328 elements, $B = 30$.

($B = 10$ in our case), computed solutions may be improve by using a finer mesh but nonetheless big magnetic fields ($B = 30, 50$ here) still give unsatisfactory results (see a plot of the solutions in Figures 2 and 3). These bad numerical results are explained by the fact that a $\mathbf{t}$-translation generates phase oscillations due to the term $\frac{B}{2}x \wedge \mathbf{t}$ in (15). With a $\mathbb{P}^1$ discretization, a necessary condition to catch the oscillations due to the coefficient $e^{i\frac{B}{2}x\wedge\mathbf{t}}$ is that the size of the space step h must be small compared to $\frac{1}{B|\mathbf{t}|}$. For a magnetic field equal to 10, Figure 2 shows quite acceptable results and

eigenvalues and moduli are close for every meshes. If we increase the magnetic field, $B = 30$, the same mesh is too coarse to catch the oscillations (see Figure 3). As soon as the translation is too large or the magnetic field too big, the fundamental state can not be determined accurately. Unfortunately, the condition $h < \frac{1}{B\mathbf{t}}$ is too restrictive since it is easily violated when B or $\mathbf{t}$ increases.

The standard method does not respect invariance properties due to gauge transformation and is inefficient to catch oscillations coming from translations of the domain. Consequently, we switch to another discretization which is not only gauge invariant, but also compatible with mesh refinement techniques. This latter property will be useful since we expect the eigenvectors to be localized on the boundary. As the phase plays an important role for both gauge transforms and domain translations, it is quite natural to decompose a function $u \in H^1(\Omega, \mathbb{C})$ into its modulus and phase

$$\forall x \in \Omega,\ u(x) = \rho(x) e^{i\theta(x)}. \tag{16}$$

As soon as $\rho \in H^1(\Omega) \cap L^\infty(\Omega)$ and $\theta \in H^1(\Omega)$, we have

$$\int_\Omega |(\nabla - iB\mathcal{A}_0)u|^2\ dx = \int_\Omega |\nabla\rho|^2 + |(B\mathcal{A}_0 - \nabla\theta)\rho|^2\ dx, \tag{17}$$

and defining the operator $P^\theta_{\mathcal{A},\Omega}$ by $P^\theta_{\mathcal{A},\Omega}\rho := -\nabla^2\rho + |\mathcal{A} - \nabla\theta|^2\rho$, we clearly have

$$P_{B\mathcal{A}_0,\Omega}(\rho e^{i\theta}) = e^{i\theta} P^\theta_{B\mathcal{A}_0,\Omega}\rho. \tag{18}$$

According to Remark 1.1, $u = \rho e^{i\theta}$ is an eigenvector with phase θ for $P_{B\mathcal{A}_0,\Omega}$ if and only if ρ is a real-valued eigenvector for $P^\theta_{B\mathcal{A}_0,\Omega}$, so, we are led to determine

$$\tilde{\mu}(B,\Omega) := \inf_{\theta\in H^1(\Omega),\ \rho\in H^1(\Omega)\cap L^\infty(\Omega),\ \rho\neq 0} \frac{\displaystyle\int_\Omega \left(|\nabla\rho|^2 + \rho^2|B\mathcal{A}_0 - \nabla\theta|^2\right)\ dx}{\displaystyle\int_\Omega |\rho|^2\ dx}. \tag{19}$$

Remark 2.3. *Comparing minimization spaces, the min-max principle gives*

$$\mu(B,\Omega) \leq \tilde{\mu}(B,\Omega). \tag{20}$$

If Ω is smooth and if the modulus ρ of the fundamental state for $P_{B\mathcal{A}_0,\Omega}$ satisfies

$$\exists C > 0,\ \forall x \in \Omega,\ \rho(x) \geq C, \tag{21}$$

then using arguments of Béthuel-Zheng [1], and Bourgain-Brezis-Mironescu [7, 8], one can show that

$$\mu(B,\Omega) = \tilde{\mu}(B,\Omega). \tag{22}$$

This relies on the uniform determination of a phase in $H^1(\Omega)$: under (21) u may be globally lifted on Ω with a phase which does not jump. Finding assumptions weaker than (21) that guarantee (22) should be investigated in the future.

Although the equality $\mu(B,\Omega) = \tilde{\mu}(B,\Omega)$ is not proved in its full generality, we use the new formulation and focus on the discretized formulation which derives naturally from (19)

$$\inf_{(\rho,\theta)\in\mathbb{P}^k(\mathcal{T}_h),\ \rho\neq 0} \frac{\displaystyle\int_\Omega \left(|\nabla\rho|^2 + \rho^2|B\mathcal{A}_0 - \nabla\theta|^2\right)\ dx}{\displaystyle\int_\Omega |\rho|^2\ dx}. \tag{23}$$

The following proposition together with performance and robustness of the new formulation (23) justify this choice.

Proposition 2.4. *The formulation (23) is gauge invariant if the gauge is in the discrete space of the phase. It is also invariant under translation or rotation of the domain as soon as this discrete space contains linear functions.*

We compute numerically $\tilde{\mu}(B,\Omega)$ by alternatively updating the phase and the modulus of the solution and beginning with minimizing the phase in (23) for an arbitrary given initial modulus. Minimizing in θ, with ρ fixed leads to minimize $J_\rho(\theta)$ given by

$$J_\rho(\theta) = \int_\Omega \rho^2 \left(|\nabla\theta|^2 - 2B\mathcal{A}_0\cdot\nabla\theta\right)\ dx, \tag{24}$$

which is equivalent to solve a second order PDE, whereas, the minimization in ρ, θ being fixed turns out to solve a classical eigenvalue problem. It is important to note that J_ρ may be degenerated precisely where ρ vanishes. However, it does not have big practical consequences on our algorithm, since if ρ is small, then u is small whatever θ is. The phase will only have a meaning where the modulus ρ is not too small.

To show the robustness of our method, we consider again the previous examples. We denote by $(\rho_j, \theta_j, \mu_h^j)_{j=0,1,2}$ the modulus, phase and energy computed for the mesh $\mathcal{T}_h^j$. Numerical results are presented in Table 2. Figures 4 and 5 give moduli and phases computed on the meshes with 138 and 1328 elements for a magnetic field $B = 30$ and 100 respectively.

Considering Table 2, it is interesting to note that the results are now coherent together: For a given mesh, the energy (and thus the eigenvalue) does not depend on the translation of the domain anymore (up to an acceptable error). Differences between coarse and fine meshes come from the

B	Mesh with 138 elements			Mesh with 1328 elements		
	$\mathcal{T}_h^0$	$\mathcal{T}_h^1$	$\mathcal{T}_h^2$	$\mathcal{T}_h^0$	$\mathcal{T}_h^1$	$\mathcal{T}_h^2$
10	4.2137	4.2153	4.2149	4.2144	4.2238	4.2166
30	12.9965	12.9964	12.9954	12.6075	12.6084	12.6092
50	22.6233	22.6232	22.6233	21.0096	21.0101	21.0107
100	49.1604	49.1604	49.1605	42.1852	42.1857	42.1858

Table 2: Smallest eigenvalues for translated meshes.

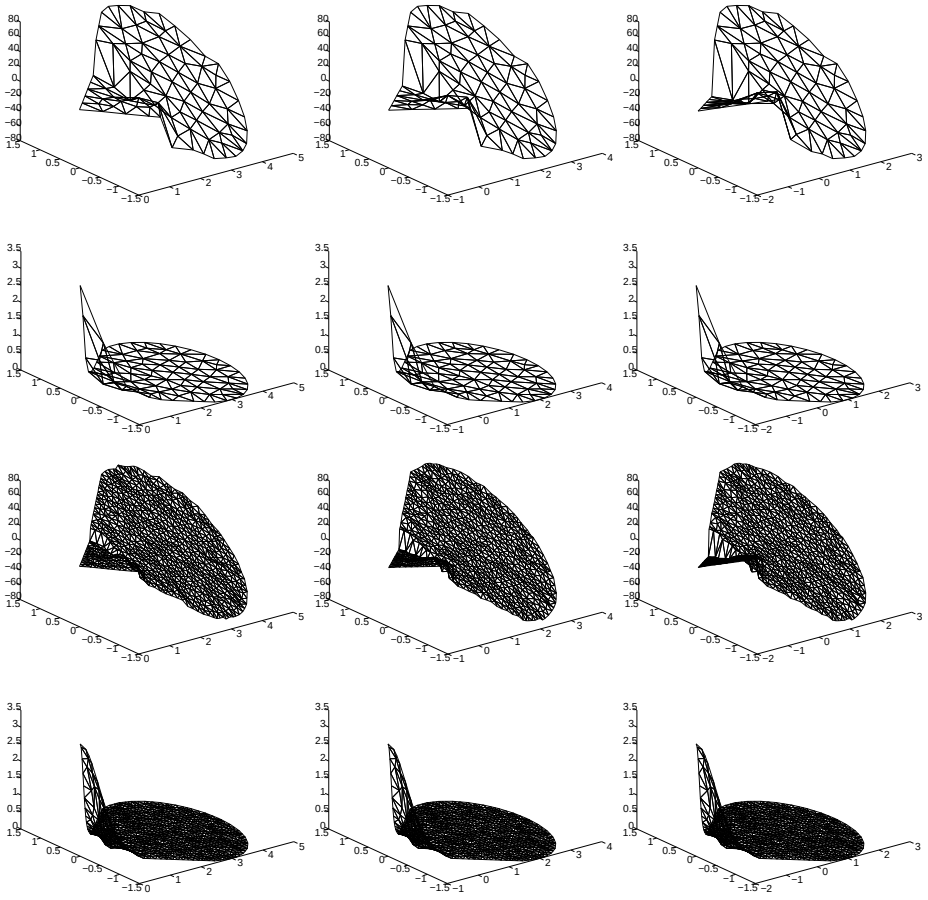

Figure 4: Phase and modulus of eigenvectors in translated meshes, B=30 and for both meshes.

bad accuracy for the coarse mesh.

We remark that the concentration of the eigenvector in the corner is faster and faster as the magnetic field B increases as illustrated in Figures 4 and 5. We also note that this new method still gives a satisfactory result for

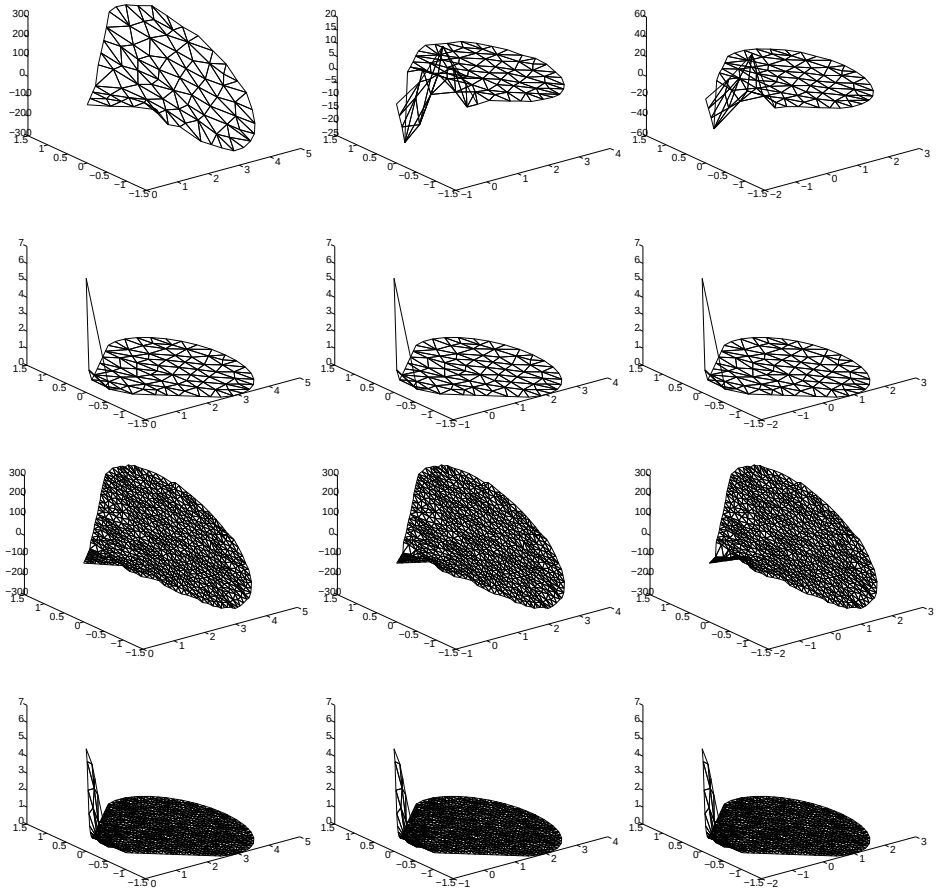

Figure 5: Phase and modulus of eigenvectors in translated meshes, B=100 and for both meshes.

intense magnetic field ($B = 100$) whereas the standard method was already inefficient from $B = 30$.

In the next section, we go one step further by implementing an a posteriori error estimate in our method. Indeed, since the eigenvector is concentrated near the boundary, we expect to refine only the relevant part of the computational domain.

3 A posteriori error estimates

We propose here to use an a posteriori error estimator which allows us to estimate the error between the exact and computed solutions only in terms of the computed solution. This estimator will be used to refine the mesh

where the numerical solution must be improved. This section is detailed in [4].

We use the same notations as Verfürth [22], p. 7-8. Let $\mathcal{T}_h$, $h > 0$ be a family of triangulations of Ω filling the following conditions:

1. Any two triangles in $\mathcal{T}_h$ share at most a common edge or a common vertex.

2. The minimal angle of all triangles in the whole family $\mathcal{T}_h$ is bounded from below by a strictly positive constant.

Let $\mathbb{P}^2(\mathcal{T}_h)$ be the classical quadratic finite element space on $\mathcal{T}_h$. We consider the following eigenvalue problem

$$\text{Find } (\mu_h, u_h) \in \mathbb{R} \times \mathbb{P}^2(\mathcal{T}_h),\ ||u_h||^2 = 1 \text{ and } \mu_h \text{ as small as possible s.t.}$$
$$p_{\mathcal{A},\Omega}(u_h, v_h) = \mu_h \langle u_h, v_h \rangle,\ \forall v_h \in \mathbb{P}^2(\mathcal{T}_h). \tag{25}$$

For any element T of the triangulation $\mathcal{T}_h$, we denote by $\mathcal{E}(T)$ and $\mathcal{N}(T)$ the set of its edges and vertices respectively and we define

$$\mathcal{E}_h := \bigcup_{T \in \mathcal{T}_h} \mathcal{E}(T), \quad \mathcal{E}_{h,\Omega} := \{E \in \mathcal{E}_h | E \subset \Omega\}.$$

For a triangle $T \in \mathcal{T}_h$ and an edge $E \in \mathcal{E}_h$, we call h_T and h_E their diameter and length, respectively. We assume that h_T, $h_E < h$.
To any edge $E \in \mathcal{E}_h$, we associate a unit vector n_E orthogonal to E (and equal to ν the unit outward normal if $E \subset \Gamma$). We also define the spaces

$$X = \mathbb{R} \times H^1_{\mathcal{A}}(\Omega) \quad \text{and} \quad X_h = \mathbb{R} \times \mathbb{P}^2(\mathcal{T}_h). \tag{26}$$

For any $(\mu, u),\ (\lambda, v) \in X$, we define

$$||(\mu, u)||_X := \left\{ |\mu|^2 + ||u||^2_{H^1_{\mathcal{A}}(\Omega)} \right\}^{1/2}, \tag{27}$$

$$\langle F(\mu, u), (\lambda, v) \rangle := \text{ Re } (p_{\mathcal{A},\Omega}(u, v) - \mu \langle u, v \rangle) + \lambda(||u||^2 - 1). \tag{28}$$

Our goal is to find $(\mu, u) \in X$ and $(\mu_h, u_h) \in X_h$ with smallest possible μ and μ_h such that

$$\forall (\lambda, v) \in X, \quad \langle F(\mu, u), (\lambda, v) \rangle = 0, \tag{29}$$
$$\forall (\lambda_h, v_h) \in X_h, \quad \langle F(\mu_h, u_h), (\lambda_h, v_h) \rangle = 0. \tag{30}$$

The following Theorem is classical and gives an a priori error estimate between the exact and numerical solutions in terms of h.

Theorem 3.1. *There exists a constant C such that for (μ, u) and (μ_h, u_h) solutions of problems (29) and (30) respectively where μ and μ_h are the smallest eigenvalues of the continuous and discrete operators, the following upper bounds hold*

$$\begin{aligned} ||u - u_h||_{H^1_{\mathcal{A}}(\Omega)} &\leq Ch, \\ |\mu - \mu_h| &\leq Ch^2. \end{aligned}$$

We now define the a posteriori error estimator for all $T \in \mathcal{T}_h$ by

$$\eta_T^2 := h_T^2 \int_T \left| -(\nabla - i\mathcal{A})^2 u_h - \mu_h u_h \right|^2 + \sum_{E \in \mathcal{E}(T) \cap \mathcal{E}_{h,\Omega}} h_E \int_E \left| [n_E \cdot (\nabla - i\mathcal{A}) u_h]_E \right|^2 . \tag{31}$$

As we see in the following theorem, η_T plays a fundamental role to estimate the local accuracy of the numerical solution.

Theorem 3.2 ([4]). *Let $(\mu, u) \in X$ and $(\mu_h, u_h) \in X_h$ be respectively solutions to (29) and (30) such that μ and μ_h are the smallest eigenvalues of the continuous and discrete operators. Then, there exist $h_0 > 0$ and constants c_1, c_2 which depend only on the regularity parameter of the triangulation such that for all $h \leq h_0$:*

$$c_1 \sum_{T \in \mathcal{T}_h} \eta_T^2 \leq |\mu - \mu_h| + ||u - u_h||^2_{H^1_{\mathcal{A}}(\Omega)} \leq c_2 \sum_{T \in \mathcal{T}_h} \eta_T^2. \tag{32}$$

Such an estimators gives a tool to improve our numerical results when coupling it with a mesh-refinement technique. Considering a tolerance ε, we refine the triangles T of $\mathcal{T}_h$ where η_T is bigger than ε. Indeed, one has from (32)

$$\varepsilon \leq \eta_T \leq \left\{ \sum_{T \in \mathcal{T}_h} \eta_T^2 \right\}^{1/2} \leq \tilde{c}_2 \left(\sqrt{|\mu - \mu_h|} + ||u - u_h||_{H^1_{\mathcal{A}}(\Omega)} \right),$$

which means that the solution is unsatisfactory.

4 Applications

We take again the example of the smoothly cut sector and a magnetic field $B = 30$. For the computations, we couple the previous estimator with an adaptive mesh refinement strategy. Table 3 gives the results for each refinement and Figure 6 shows the mesh after six refinements and gives the computed phase and the modulus.

We observe that the refinement takes place essentially near the corner and also near the boundary. This is in perfect agreement with results of

refinement	number of elements	number of degrees of freedom	η	μ_h
1	38	101	38.993385	15.572444
2	102	235	22.828768	13.815911
3	206	459	9.037603	12.826912
4	394	855	5.857042	12.670129
5	800	1699	2.240146	12.638226
6	1726	3593	0.792354	12.628898
7	3807	7826	0.272165	12.627361
8	8219	16742	0.104900	12.626788
9	15517	31446	0.060877	12.626605

Table 3: Results for the adaptive method, $B = 30$.

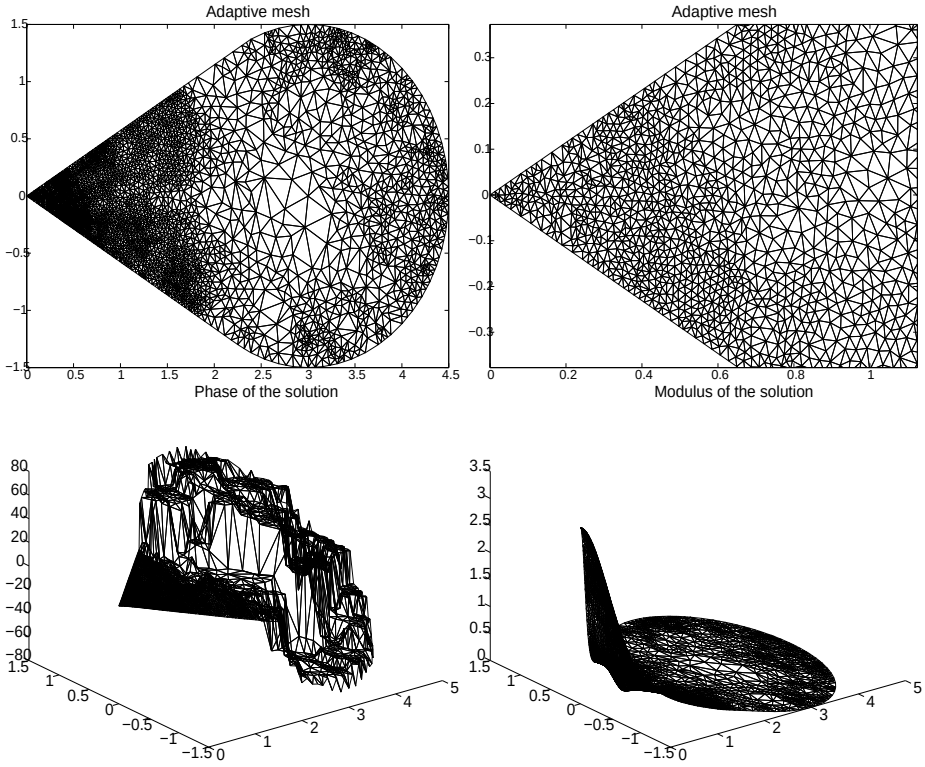

Figure 6: Solution for the sixth refinment, $B = 30$.

localization announced by [3].

When comparing the adaptive mesh refinement method (Table 3) to a uniform mesh refinement (Table 4), we see that the former is more reliable

and faster than the uniform method. Moreover, its power and robustness become bigger and bigger when the magnetic field is increased since the solution is more and more concentrated near the boundary as illustrated in Figure 7.

refinement	number of elements	number of degrees of freedom	η	μ_h
1	38	101	39.711605	15.569330
2	48	125	22.754814	13.816984
3	70	171	14.493879	13.440501
4	193	428	8.227542	12.826351
5	522	1113	4.960995	12.687395
6	1349	2790	2.059195	12.641156
7	3593	7350	0.772448	12.630521
8	9583	19448	0.279150	12.627457

Table 4: Results for the uniform mesh refinement method, $B = 30$.

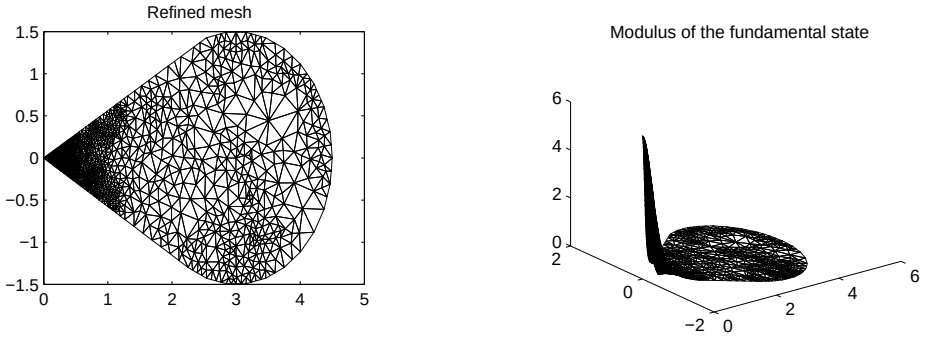

Figure 7: Solution for $B = 100$.

As we have already seen, adaptive mesh refinement is well adapted to determine accurate numerical solution for problem (6). We propose to use our algorithm to analyze the behavior of $\mu(\alpha)$ according to the angle α numerically. Before this, let us just recall that this behavior is theoretically

unknown but the following estimates hold (see [3]):

$$\forall \alpha \in]0, 2\pi[, \ \mu(\alpha) \leq \Theta_0, \tag{33}$$

$$\forall \alpha \in]0, \pi[, \ \mu(\alpha) \geq \Theta_0 \frac{\alpha}{\pi}, \tag{34}$$

$$\forall \alpha \in]0, 2\pi[, \ \mu(\alpha) \leq \frac{\alpha}{\sqrt{3}}, \tag{35}$$

$$\lim_{\alpha \to 0} \frac{\mu(\alpha)}{\alpha} = \frac{1}{\sqrt{3}}. \tag{36}$$

Since Ω_α is invariant under dilatation, we know according to Remark 2.1 that $\mu(B, \Omega_\alpha) = B\mu(\alpha)$. In order to approximate $\mu(\alpha)$, we consider the previous angular sector and cut-off by a piece of circle so that the boundary is still smooth, except at the corner. The bottom of the spectrum does not change (with an exponentially small error due to the exponential decay away the corner, cf. [3]) if the cut-off is sufficiently far from the corner. The smooth cut-off does not introduce any new superconducting point and therefore does not change the superconducting properties of the sample. Numerical estimates of $\mu(\alpha)$ are given in Figure 8. We note that they are in perfect agreement with estimates (33), (34), (35) and (36): the asymptotics near zero is conserved and numerical results convince us that μ is increasing from $]0, \pi]$ onto $]0, \Theta_0]$.

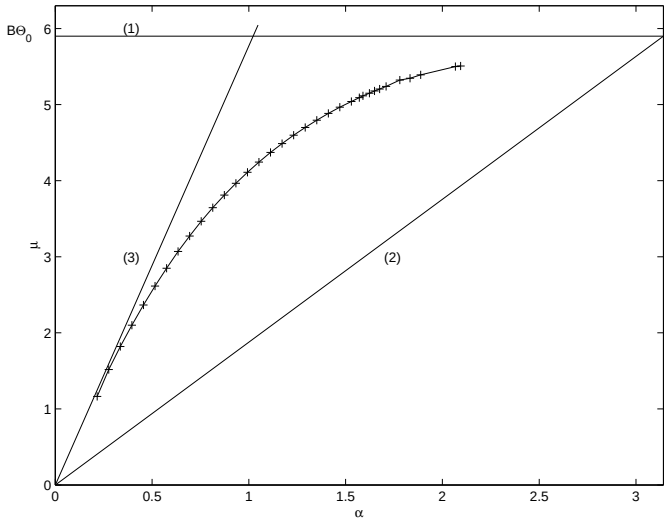

Figure 8: Theoretical and numerical estimates of $\mu(\alpha)$, $B = 10$.

We now briefly treat two domains for which we apply the adaptive mesh refinement algorithm. It is interesting to observe in Figure 9 that the localization takes place at the corner with smallest angle. We notice that

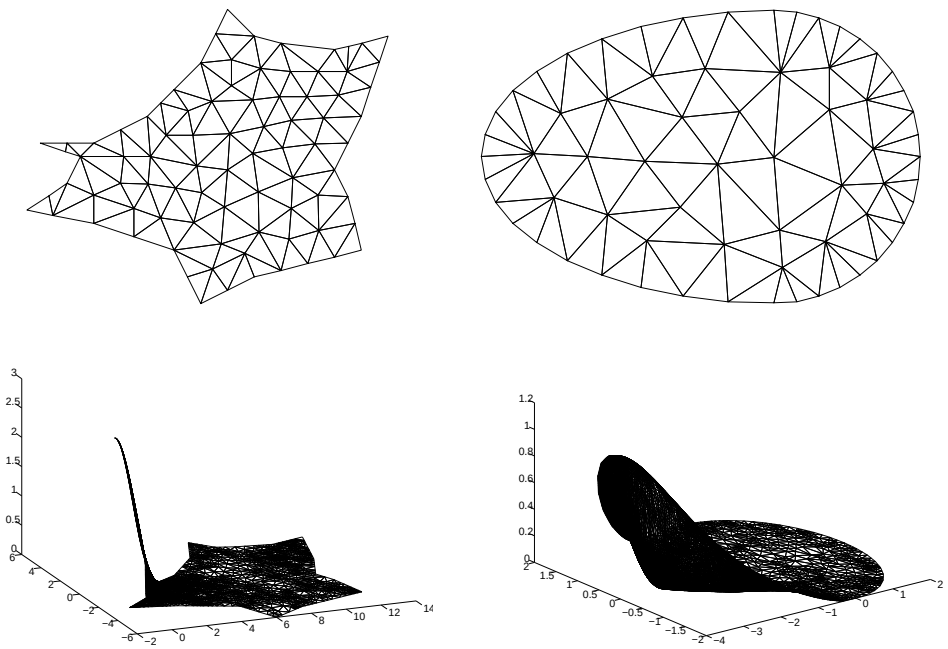

Figure 9: Superconductivity in general domains.

the second domain is smooth and our result illustrates those obtained by Helffer-Morame [13] which states that the first eigenvector is localized at points of the boundary with maximal curvature.

5 Conclusion

We have proposed here a robust and powerful method to compute fundamental states associated to the Schrödinger operator with constant magnetic field, and couple this method with an adaptive mesh refinement technique deduced from the construction of an a posteriori error estimate. The numerical method enables us to estimate $\mu(\alpha)$, the bottom of the spectrum for the Schrödinger operator with a constant magnetic field in a sector of $\mathbb{R}^2$ with angle α. These numerical estimates coupled with results of [3, 5] let us suggest that the first eigenfunction of the Schrödinger operator with magnetic field is exponentially localized in the smallest corners of the boundary of the domain and $\mu(\alpha)$ is increasing with α.
In domain with several minimal angles, multiple solutions may appear as explained in [5] and [6] where a different numerical approach based on an high order finite element method is used.

References

[1] Bethuel, F., and Zheng, X. M. Sur la densité des fonctions régulières entre deux variétés dans les espaces de Sobolev. *C. R. Acad. Sci. Paris Sér. I Math. 303*, 10 (1986), 447–449.

[2] Bonnaillie, V. *Analyse mathématique de la supraconductivité dans un domaine à coins; méthodes semi-classiques et numériques*. Thèse de doctorat, Université Paris XI - Orsay, 2003.

[3] Bonnaillie, V. On the fundamental state energy for a Schrödinger operator with magnetic field in domains with corners. *Asymptot. Anal. 41*, 3-4 (2005), 215–258.

[4] Bonnaillie Noël, V. A posteriori error estimator for the eigenvalue problem associated to the Schrödinger operator with magnetic field. *Numer. Math. 99*, 2 (2004), 325–348.

[5] Bonnaillie Noël, V., and Dauge, M. Asymptotics for the low-lying eigenstates of the Schrödinger operator with magnetic field near corner. *In preparation* (2005).

[6] Bonnaillie Noël, V., Dauge, M., Martin, D. and Vial, G. Computations of the first eigenpairs for the Schrödinger operator with magnetic field. *In preparation* (2005).

[7] Bourgain, J., Brezis, H., and Mironescu, P. On the structure of the Sobolev space $H^{1/2}$ with values into the circle. *C. R. Acad. Sci. Paris Sér. I Math. 331*, 2 (2000), 119–124.

[8] Bourgain, J., Brezis, H., and Mironescu, P. Limiting embedding theorems for $W^{s,p}$ when $s \uparrow 1$ and applications. *J. Anal. Math. 87* (2002), 77–101. Dedicated to the memory of Thomas H. Wolff.

[9] Brosens, F., Devreese, J. T., Fomin, V. M., and Moshchalkov, V. V. Superconductivity in a wedge : analytical variational results. *Solid State Comm. 111*, 2 (1999), 565–569.

[10] De Gennes, P. G. *Superconductivity in metals and Alloys*. Addison Wesley, 1989.

[11] Fomin, V. M., Devreese, J. T., and Moshchalkov, V. V. Surface superconductivity in a wedge. *Europhys. Lett. 42*, 5 (1998), 553–558.

[12] Helffer, B., and Mohamed, A. Semiclassical analysis for the ground state energy of a Schrödinger operator with magnetic wells. *J. Funct. Anal. 138*, 1 (1996), 40–81.

[13] Helffer, B., and Morame, A. Magnetic bottles in connection with superconductivity. *J. Funct. Anal. 185*, 2 (2001), 604–680.

[14] Helffer, B., and Pan, X.-B. Upper critical field and location of surface nucleation of superconductivity. *Ann. Inst. H. Poincaré, Anal. Non Linéaire 20*, 1 (2003), 145–181.

[15] Hornberger, K., and Smilansky, U. The boundary integral method for magnetic billiards. *J. Phys. A 33*, 14 (2000), 2829–2855.

[16] Jadallah, H. T. The onset of superconductivity in a domain with a corner. *J. Math. Phys. 42*, 9 (2001), 4101–4121.

[17] Lu, K., and Pan, X.-B. Estimates of the upper critical field for the Ginzburg-Landau equations of superconductivity. *Phys. D 127*, 1-2 (1999), 73–104.

[18] Lu, K., and Pan, X.-B. Gauge invariant eigenvalue problems in $\mathbf{R}^2$ and in $\mathbf{R}^2_+$. *Trans. Amer. Math. Soc. 352*, 3 (2000), 1247–1276.

[19] Pan, X.-B. Upper critical field for superconductors with edges and corners. *Calc. Var. Partial Differential Equations 14*, 4 (2002), 447–482.

[20] Schweigert, V. A., and Peeters, F. M. Influence of the confinement geometry on surface superconductivity. *Phys. Rev. B 60*, 5 (1999), 3084–3087.

[21] Tinkham, M. *Introduction to superconductivity.* McGraw Hill, 1996.

[22] Verfürth, R. *A review of a posteriori error estimation and adaptive mesh refinement technique.* Wiley Teubner, 1996.